Acta Cryst. (1998). A**54**, 225–231

Standard Uncertainty of Angular Positions and Statistical Quality of Step-Scan Intensity Data

C. Rebmann, H. Ritter and J. Ihringer*

Institut für Kristallographie der Universität Tübingen, Charlottenstrasse 33, D-72070 Tübingen, Germany. E-mail: joerg.ihringer@uni-tuebingen.de

(*Received 17 February 1997; accepted 20 October 1997*)

Abstract

In step-scan diffraction measurements, the diffraction angle 2θ is an observation with standard uncertainty $u(2\theta)$. By the law of uncertainty propagation, $u(2\theta)$, typically $0.001 < u(2\theta) < 0.004°$, affects the standard uncertainty $u_{\rm total}(y)$ of the intensity y at each step $2\theta_i$, depending on the local slope $y'_i = {\rm d}y/{\rm d}(2\theta)|_{2\theta_i}$, by $u^2_{\rm total}(y_i) = u^2_{\rm Poisson} + [y'_i u(2\theta)]^2$, where $u_{\rm Poisson} = (y_i)^{1/2}$ is the conventional Poisson statistics. For the intensity y at 2θ of steepest slope, $u_{\rm total}(y)$ is given by $u^2_{\rm total}(y) = u^2_{\rm Poisson}(1 + v^2)$, where $v = 2u(2\theta){y_0}^{1/2}/h$ is the ratio of $y'_i u(2\theta)$ and $u_{\rm Poisson}$, y_0 is the peak intensity and h the full width at half-maximum of the profile. The error of the intensities at individual steps modifies also the standard uncertainty of the integrated intensity: $u^2_{\rm total}({\rm Int}) = u^2_{\rm Poisson}({\rm Int})(1 + v^2/2)$. As v depends on $y_0^{1/2}/h$, it is evident that the importance of the correction increases with increasing count rates and decreasing line width. In most practical cases, $y'_i u(2\theta)$ contributes a multiple of Poisson statistics to the standard uncertainty of intensity. It will be shown that with a realistic weighting scheme the χ^2 as well as the Durbin–Watson test become more meaningful.

1. Introduction

Statistical validity of the standard uncertainty of intensity data is a necessity for the successful structure determination by least-squares refinement or maximum-entropy methods. Concerning powder data, Sakata & Cooper (1979) found that the standard uncertainties of parameters in full-profile refinements by the Rietveld method (Rietveld, 1967, 1969) are usually underestimated by at least a factor of two compared with parameters deduced from single-crystal data. A systematic research into the question of the effect of profile step counting time and of the profile step width on the structural parameters and their standard uncertainty followed by Hill & Madsen (1984, 1986). Flack & Vincent (1980) suggested the application of a quantitative test for serial correlation, published by Durbin & Watson (1950, 1951, 1971), to single-crystal intensity data. Hill & Madsen (1986) applied this test to optimize the profile step width. A review of the use of the Durbin–Watson test applied to the Rietveld analysis was given by Hill & Flack (1987). Bérar & Lelann (1991) suggested a modification of the least-squares procedure to reduce the influence of serial correlation on the standard uncertainty of the structural parameters. Some general comments on the question of statistical validity in the Rietveld method are summarized by Willis & Albinati (1992) and by Prince (1993). The fundamentals of the statistical descriptors including the goodness of fit and weighting schemes used in crystallography are given by Schwarzenbach *et al.* (1989). In this paper, we focus on the statistical quality of step-scan data, that is, on the intensities y_i and the angles $2\theta_i$ for each step i.

In profile refinement, each observed intensity $y^{\rm obs}$ is assigned to a 2θ value, which is a real number with a standard uncertainty $u(2\theta)$ given by the mechanical precision of the instrument. However, in most data-evaluation programs, 2θ is calculated under the condition of a constant step width and the error of the position is ignored. The latter is independent of the standard uncertainty of the count rate y_i, given by Poisson statistics $u_{\rm Poisson} = {y_i}^{1/2}$. Therefore, the total variance of the intensity y_i at step i may be calculated by uncertainty propagation:

$$u^2_{\rm total}(y_i) = u^2_{\rm Poisson} + [y'_i u(2\theta)]^2, \qquad (1)$$

with $y'_i = {\rm d}y/{\rm d}(2\theta)|_{2\theta_i}$, the local slope of the intensity profile at step i, position $2\theta_i$ (Lehmann *et al.*, 1987; Ihringer, 1995*a*).

In the following, we analyse systematically the impact of a modified weighting scheme on the refinement results by repeated experiments. It includes, as given above, the Poisson statistics for the intensities and an assumption of a Gaussian distribution of the observed 2θ angle around its mean value.

2. Experimental

Repeated measurements of four different reflections are the basis for the subsequent statistical analysis. They were carried out on two automated Guinier diffractometers (Ihringer & Appel, 1984; Ihringer & Röttger, 1993, 1994, 1997) both mounted on line-focus windows of a rotating-anode generator with a copper target (fine

© 1998 International Union of Crystallography
Printed in Great Britain – all rights reserved

ISSN 0108-7673 © 1998

Table 1. *Summary of experimental details*

FWHM and peak intensity y_0 are mean values of all measurements of the corresponding reflection. n is the number of repetitions.

Sample	Reflection	Step range (°2θ)	FWHM (°)	y_0	n
Silicon †	220	46.75–47.75	0.080	13170	447
Silicon †	311	55.5–56.5	0.084	6960	585
Silicon †	331	75.58–76.58	0.100	3464	585
$PbSO_4$‡	201	49.5–49.98	0.081	5473	580

† 51 steps, counting time 30 s, step width $\Delta 2\theta$ = 0.02°2θ. ‡ 25 steps, counting time 10 s, step width $\Delta 2\theta$ = 0.02°2θ.

focus 0.3 × 3 mm, 45 kV, 80 mA). Monitor counters behind each of the Ge (111) monochromators, adjusted for $K\alpha_1$ radiation, controlled the primary-beam intensity. Details of the measurements are given in Table 1.

3. Data evaluation

3.1. *Qualifier for the refinement results*

For each profile, the correspondence of the n ($n = 51$ for the Si 220, 311, 331, $n = 25$ for the $PbSO_4$ 201 reflections) measured intensity data $y_i^{\rm obs}$, their standard uncertainties u_i and the calculated intensities for the model of the profile with p parameters defined for example in equations (3)–(7) is quantified by the magnitude of $M = \sum_{i=1}^{n}[(y_i^{\rm obs} - y_i^{\rm calc})^2/u_i^2]$. The significance level of M may be determined applying the χ^2 test for $\nu = n - p$ degrees of freedom or, more directly, by calculating $N_\sigma = (M - \nu)/(2\nu)^{1/2}$ (Parrish & Wilson, 1992; Ihringer, 1995*b*), where $N_\sigma < 3$ is expected when the model fits the data and their standard uncertainties.

More significant than a single value of M is its distribution for repeated measurements of the same reflection because it approaches the χ^2 distribution for ν degrees of freedom supposing that model, data and standard uncertainties are correct. Thus, we compare the distribution of M with the χ^2 distribution in three different cases to judge the validity of the assumed standard uncertainties. As a qualifier for a whole series of experiments, we use the average value $\overline{N_\sigma}$, given in all figures, $\overline{N_\sigma} = (1/447)\sum_{\mu=1}^{447} N_\sigma^\mu$. N_σ^μ is calculated for the $\mu = 1, \ldots, 447$ scans of Si 220 as well as for profiles given in Table 1.

3.2. *Intensity of the focused primary beam*

The monitor counters at both Guinier diffractometers are fixed downstream of the monochromator perpendicular to the beam path and record the diffuse radiation scattered from a polyamide foil. We used these data to verify the validity of Poisson statistics for a fixed counter arrangement. For each of the $\mu = 1, \ldots, 447$ measurements of the Si 220 reflection, the qualifier M_μ is calculated:

$$M_\mu = \sum_{i=1}^{n}(y_i^{\rm mon} - \overline{y_\mu^{\rm mon}})^2/u_i^2. \qquad (2)$$

The observed intensity $y_i^{\rm mon}$ is the monitor count collected during the constant measuring time of 30 or 10 s, respectively (see Table 1), at each of the $i = 1, \ldots, n$ steps of the profile with standard uncertainty $u_i = (y_i^{\rm mon})^{1/2}$. The calculated intensity $\overline{y_\mu^{\rm mon}}$ is the mean value of the monitor rate during n steps, that is, the model assumes constant primary radiation during the measuring time for a profile. Fig. 1 shows the distribution of the M_μ values for all 447 profiles of the Si 220 reflection together with the χ^2 distribution for 50 degrees of freedom, as there are 51 measurements within one profile and the model – constant intensity – consists of 1 parameter.

It is evident that M for most of the profiles lies within the χ^2 distribution, but some are too high. M outside the χ^2 distribution means that within the measuring time for a profile (typically 25 min) the monitor count rate deviated more from its mean value than expected by Poisson statistics. Nevertheless, we dare to conclude from Fig. 1 that in most cases the assumption of a constant primary-beam intensity with Poisson statistics is justified, even if $\overline{N_\sigma} = 6.3$.

3.3. *Models for the profile*

Next, each of the 447 scans of the Si 220 reflection was refined using five different models for the profile:

(i) Lorentzian (L) with three parameters:

$$L(x_{iK}, h_K, I_K) = I_K(2/\pi h_K)[1/(1 + x_{iK}^2)]. \qquad (3)$$

(ii) Gaussian (G) with three parameters:

$$G(x_{iK}, h_K, I_K) = I_K\{[2(\ln 2)^{1/2}]/(h_K\pi^{1/2})\} \times \exp[-(\ln 2)x_{iK}^2]. \qquad (4)$$

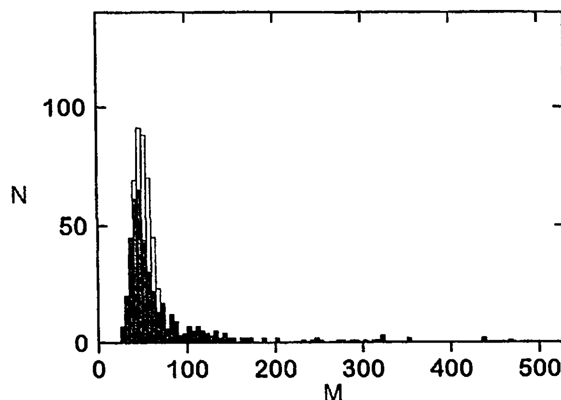

Fig. 1. Histogram of M (full) calculated with the monitor count rate assuming constant intensity within the 51 steps of a profile, standard uncertainties from Poisson statistics and χ^2 distribution (light) for 50 degrees of freedom, $\overline{N_\sigma} = 6.3 \pm 1.4$.

(iii) Pseudo-Voigt (PV) with four parameters:

$$\mathrm{PV}(x_{iK}, h_K, I_K, \eta) = \eta L(x_{iK}, h_K, I_K) + (1-\eta)\, G(x_{iK}, h_K, I_K). \quad (5)$$

(iv) Pseudo-Voigt + Gaussian (PV + G) with seven parameters:

$$\mathrm{PV} + G = \eta L(x_{iK}, h_K, I_K) + (1-\eta)\, G(x_{iK}, h_K, I_K) + G(x'_{iK}, h'_K, I'_K) \quad (6)$$

(v) Two pseudo-Voigts (PV_1 + PV_2) with eight parameters:

$$PV_1 + PV_2 = \eta L(x_{iK}, h_K, I_K) + (1-\eta)\, G(x_{iK}, h_K, I_K) + \eta' L(x'_{iK}, h'_K, I'_K) + (1-\eta')\, G(x'_{iK}, h'_K, I'_K) \quad (7)$$

(Young, 1993).

All functions are given for the integrated intensity I_K with argument $x_{iK} = (2\theta_i - 2\theta_K)(2/h_K)$ for step i at angle $2\theta_i$, where $2\theta_K$ is the position of the Kth reflection and h_K is the full width at half-maximum (FWHM). Two additional parameters were used in each case for a straight-line background.

3.4. *Si 220 reflection with pseudo-Voigt profile function*

The histogram of M for the model with one pseudo-Voigt function (3) with standard uncertainties calculated from Poisson statistics only is given in Fig. 2(a) together with the corresponding χ^2 distribution for $\nu = 45$ degrees of freedom. It is easy to see and confirmed by the mean value of $\overline{N_\sigma} = 23.3$ that the M distribution is quite different from the χ^2 distribution. For the pure Gaussian or Lorentzian profiles, the agreement is even worse.

For the histogram in Fig. 2(b), the standard uncertainties are modified by an *Ansatz* including a Gaussian-distributed error for 2θ with $u(2\theta) = 0.001°$. The value 0.001° may be seen as a lower limit of the mechanical accuracy of the gear: $0.001 < u(2\theta) < 0.005°$. The uncertainty propagation $u^2_{\text{total}} = u^2_{\text{Poisson}} + [y'_i u(2\theta)]^2$ is calculated using

$$y'_i = \overline{y_0}' = (1/12h)(y_{-2} - 8y_{-1} + 8y_1 - y_2) \quad (8)$$

with the step width h. From Fig. 2(b), it is evident that the M distribution fits χ^2 much better than in Fig. 2(a) and $\overline{N_\sigma}$ decreases to 6.5, which is still too high.

3.5. *Variation of the weighting scheme*

Best coincidence between the M and the χ^2 distributions is obtained with $u(2\theta) = 0.00375°$, which yields $\overline{N_\sigma} = -0.06$, see Fig. 2($c$). This value was found from a variation of the assumed gear accuracy $u_k(2\theta) = k \times 0.00025°$ (k = 0, ..., 27) by calculating 28 distributions M_k for different $u_k(2\theta)$. For each k, a qualifier M'_k is defined by

$$M'_k = \sum_{i=1}^{r} (n_i - np_i)^2 / np_i, \quad (9)$$

which measures the coincidence between the M_k and the χ^2 distribution. Both distributions are shown in Fig. 2 for

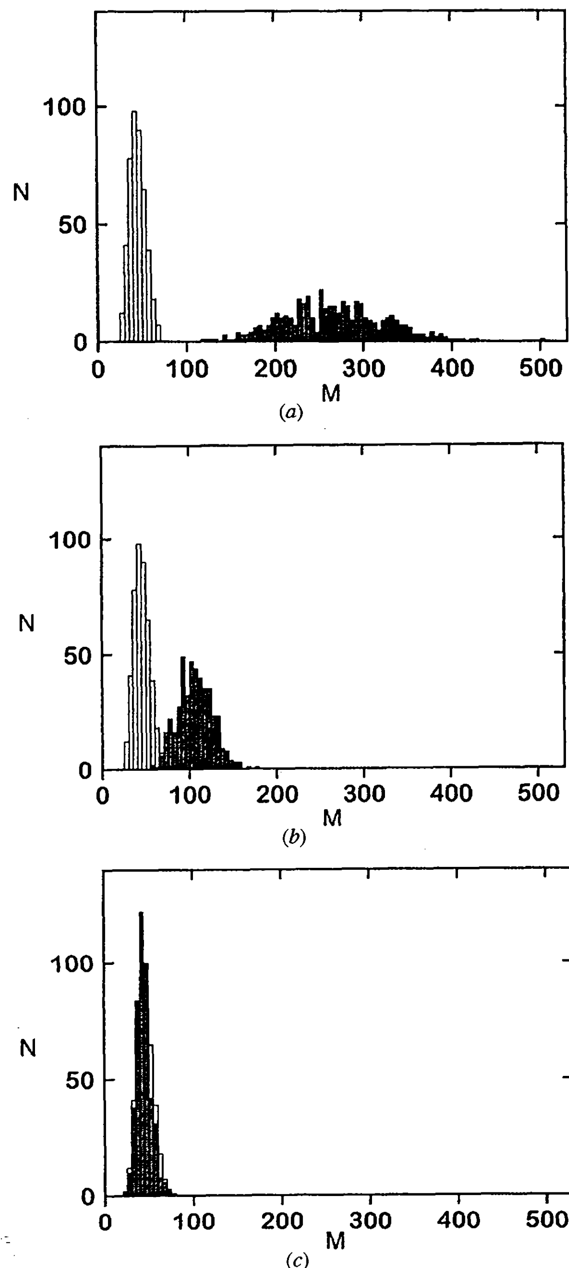

Fig. 2. Histogram of M (full) for 447 silicon 220 reflections refined by pseudo-Voigt profiles and χ^2 distribution (light) for 45 degrees of freedom. M calculated with: (a) standard uncertainties from Poisson statistics only [$u(2\theta) = 0°$], $\overline{N_\sigma} = 23.3 \pm 0.3$; ($b$) standard uncertainties calculated using equation (1) with $u(2\theta) = 0.001°$, $\overline{N_\sigma} = 6.5 \pm 0.1$; ($c$) standard uncertainties calculated from equation (1) with $u(2\theta) = 0.00375°$, $\overline{N_\sigma} = -0.06 \pm 0.04$.

Table 2. *Mean value of N_σ for various reflections (see Table 1) for each of the profile functions calculated with $u(2\theta) = 0$ and $u(2\theta) = 0001°$, respectively [equation (1)]*

The $PbSO_4$ reflection was asymmetric.

Profile	Si 220	Si 311	Si 331	$PbSO_4$ 201	$u(2\theta)$ (°)
Lorentz (*L*)	263±1.8	120±0.7	47.0±0.4	115.0±0.5	0
Gauss (*G*)	173±1.5	109±0.5	42.8±0.2	145.0±0.8	
PV	23±0.3	15±0.2	3.9±0.08	80.8±0.5	
PV+*G*	2.5±0.09	1.9±0.1	1.4±0.06	8.3±0.1	
PV_1+PV_2	1.1±0.06	0.4±0.05	0.4±0.05	8.1±0.1	
Lorentz (*L*)	85±1	57.3±4	33.2±0.3	72.0±0.3	0.001
Gauss (*G*)	115±1	82.5±3	37.3±0.2	95.1±0.4	
PV	6.5±1	6.0±0.08	2.3±0.06	50.1±0.2	
PV+*G*	1.2±0.6	0.6±0.06	0.8±0.05	4.2±0.08	
PV_1+PV_2	0.1±0.05	−0.1±0.04	0.1±0.05	4.7±0.09	

$u_k = 0, 0.001, 0.00375°$: the full histogram gives the frequency n_i of M_k in the interval i and the light histogram shows its theoretical value np_i calculated for the total number of n values M_k by

$$p_i = \int_{x_{i-1}}^{x_i} \chi^2(x)\,dx. \qquad (10)$$

The abscissa is divided into intervals of size 5. The weights np_i follow from Poisson statistics for the frequency in each interval. For the optimal $u_k(2\theta)$, M' is expected to be the number of degrees of freedom $r - 1$. The quantitative measure

$$N'_\sigma = [M' - (r-1)]/[2(r-1)]^{1/2} \qquad (11)$$

calculated for the 28 different values of $u_k(2\theta)$ and r intervals of size 2 is given in Fig. 3. It exhibits best coincidence of the M_k and χ^2 distributions by the minimum of $N'_\sigma = 1.7$ at $u(2\theta) = 0.00375°$. The magnitude of $u(2\theta)$ is in good agreement with the standard uncertainty for the gears given by the manufacturing firm.

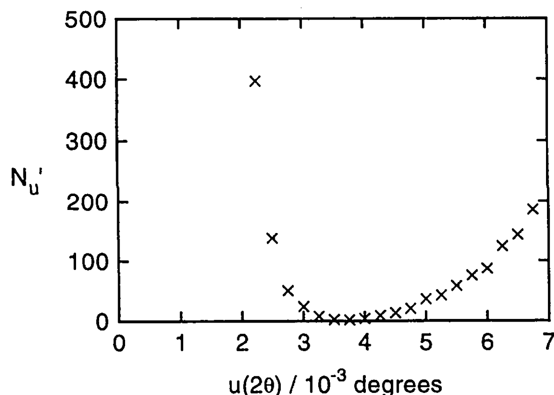

Fig. 3. N'_σ giving the difference between the M and the χ^2 distribution (see Fig. 2) as a function of the standard uncertainty of the angle position. $u(2\theta) = 0.00375°$ yields the best fit.

3.6. *Si 220, Si 113, Si 331 and $PbSO_4$ 201 reflections with different models for the profile*

The analysis given here in detail for the Si 220 data refined with the pseudo-Voigt profile model was repeated with all profile functions for the Si 311, Si 331 and $PbSO_4$ 201 reflections. Table 2 summarizes the results for $u(2\theta) = 0°$ and $u(2\theta) = 0.001°$.

A comment should be given for profiles PV + *G* and $PV_1 + PV_2$: each of them is a combination of two curves. From Table 2, it is evident that they fit best to all of the profiles. However, it should be noted that, for the refinement of *e.g.* the Si 220 reflection with profile $PV_1 + PV_2$, all eight parameters consisting of two sets η, x_{iK}, h_K, I_K for the two pseudo-Voigt functions have been recalculated for each of the 447 reflections. So, variations in shape between subsequent profiles are compensated by variation of the individual parameter sets for the two contributing profiles PV_1 and PV_2. In the analysis given here, even the single pseudo-Voigt function is more flexible than in the Rietveld refinement, as we recalculated η and FWHM for each of the 447 Si 220 reflections, whereas in Rietveld refinement all profiles within a diffraction diagram share the same η value and FWHM function.

3.7. *Durbin Watson d and N_σ for the Si 220 reflection*

This section gives the analysis of the impact of the modified weighting scheme upon the Durbin–Watson qualifiers, which are used as indicators for serial correlation. First, for each of the 447 Si 220 reflections using a pseudo-Voigt function, d and Q were calculated for a significance level of $p = 3$ (Flack & Vincent, 1980). Fig. 4 exhibits the result for $u(2\theta) = 0°$ (*a*) and $u(2\theta) = 0.0035°$ (*b*).

For $u(2\theta) = 0°$, Fig. 4(*a*) shows $d > Q$ for most of the profiles, so the Durbin–Watson test judges observed and calculated data as free from serial correlation. With $u(2\theta) = 0.0035°$, however, there is serial correlation for nearly 30% of the profiles (Fig. 4*b*), even if the model, a single symmetric pseudo-Voigt function [equation (5)],

was not changed. To decide if this is an artifact, we repeated the analysis with the same data but with the most flexible function $PV_1 + PV_2$ [equation (7)], which fits asymmetric profiles too and yields perfect refinement even with $u(2\theta) = 0°$ (see Table 2). It follows that $d > Q$, no serial correlation, for all data independent of the weighting scheme. Evidently, in the refinement with one single pseudo-Voigt function, the minor asymmetry in some of the Si 220 profiles is blurred by weighting with Poisson statistics only. However, with the more realistic weighting scheme, the statistic tests become more susceptible to differences between observed and calculated data.

The plot of N_σ *versus* Durbin–Watson d for 447 Si 220 reflections (Fig. 4 bottom) shows that there is no correlation between the two quantities. Changing the weighting scheme with $u(2\theta) = 0.0035°$ affects mainly N_σ, it decreases from 30 to 6. The d distribution becomes broadened and, with the single pseudo-Voigt model, shifted in the direction indicating positive serial correlation.

4. Discussion

4.1. *Standard uncertainty of the intensity at the angle of steepest ascent*

By the law of uncertainty propagation, $u(2\theta)$ contributes to the square of the standard uncertainty $u^2_{\rm total}(y)$ of the intensity y [see equation (1)]. To estimate the magnitude of $[y_i'u(2\theta)]^2$ compared with $u^2_{\rm Poisson}$ calculated from Poisson statistics only, we define the ratio

$$v = y_i'u(2\theta)/u_{\rm Poisson} \qquad (12)$$

and determine its maximum value, which is reached where the profile shows its steepest slope [equation (1)].

If a Gaussian profile is assumed,

$$y = y_0 \exp[-(4\ln 2/h^2)x^2] \quad (x = 2\theta - 2\theta_0), \qquad (13)$$

$x_s = 2\theta_s - 2\theta_0$ follows from the condition for steepest slope,

$$\left.\frac{d^2y}{dx^2}\right|_{x_s} = 0, \qquad (14)$$

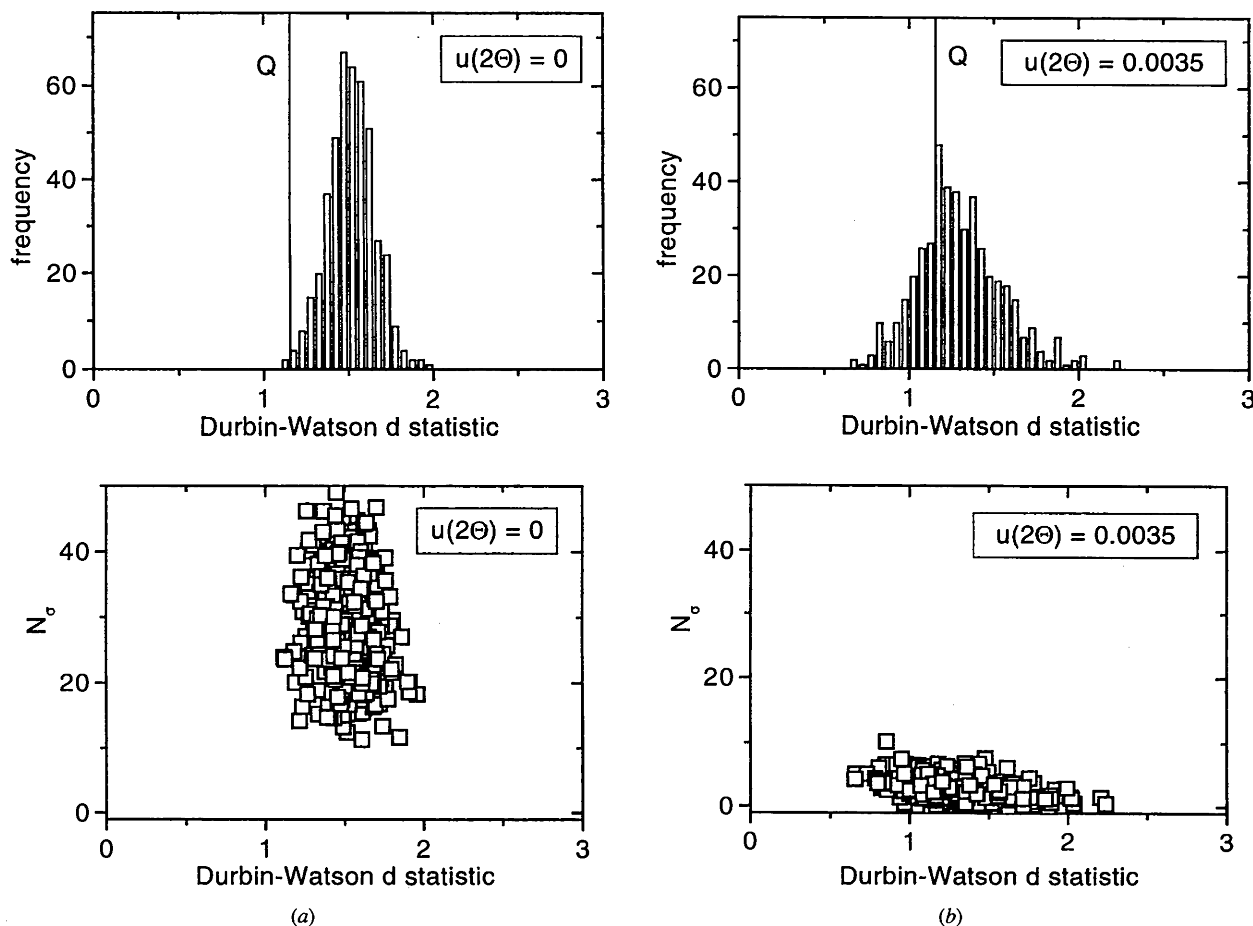

Fig. 4. Durbin–Watson statistic for 447 Si 220 profiles. (*a*) $u(2\theta) = 0°$. (*b*) $u(2\theta) = 0.0035°$. Upper diagrams: Distribution of the Durbin–Watson d values and Q for significance = 0.1%. Bottom: Durbin–Watson d *versus* N_σ.

to give

$$x_s = h/2(2\ln 2)^{1/2}. \tag{15}$$

Inserting x_s into (12) gives the ratio v as

$$\begin{aligned} v &= \left[\frac{dy}{dx}\bigg|_{x_s} u(2\theta)\right] \bigg/ u_{\text{Poisson}} \\ &= \left[\frac{dy}{dx}\bigg|_{x_s} u(2\theta)\right] \bigg/ [y(x_s)]^{1/2} \\ &= (8\ln 2)^{1/2} {y_0}^{1/2} \exp(-\tfrac{1}{4}) u(2\theta)/h \\ &\approx (2{y_0}^{1/2}/h) u(2\theta) \end{aligned} \tag{16}$$

and the total standard uncertainty becomes

$$u^2_{\text{total}}(y) = u^2_{\text{Poisson}}(1 + v^2). \tag{17}$$

The ratio v, which is dependent on the peak intensity y_0 for some characteristic values for FWHM h and for $u(2\theta) = 0.005°$, is given in Fig. 5. For $v < 1$, $u(2\theta)$ may be omitted, however, as FWHM is less than 0.1° for most instruments, $v < 1$ holds for a profile with peak intensities below 500 only. At a synchrotron source, with FWHM = 0.025°, *e.g.* even for a profile with low peak intensity of 500 counts Fig. 5 shows that $y_i' u(2\theta)$ is nine times the standard uncertainty from Poisson statistics u_{Poisson}. From Fig. 5, it might be seen that, when $y_0 > 2000$, even for broad profiles (FWHM ≈ 0.2°2θ), the contribution of $y_i' u(2\theta)$ becomes more than twice that of u_{Poisson}.

4.2. *Standard uncertainty of integrated intensity*

The standard uncertainty of the angular position $u(2\theta)$ does not only affect the standard uncertainty of the count rate collected at a certain angle but also the standard uncertainty of the integrated intensity of a reflection. For the integrated intensity

$$I = \sum_{i=1}^{n} y_i^{\text{obs}} \tag{18}$$

for n steps over the profile, the standard uncertainty including $u(2\theta)$ is

$$\begin{aligned} u^2_{\text{total}}(\text{Int}) &= u^2_{\text{Poisson}}(\text{Int}) + \sum_{i=1}^{n} [y_i' u(2\theta)]^2 \\ &= \sum_{i=1}^{n} y_i^{\text{obs}} + \sum_{i=1}^{n} [y_i' u(2\theta)]^2. \end{aligned} \tag{19}$$

An analytical expression follows when the sums are replaced by integrals and the intensities are approximated by Gaussian profiles:

$$u^2_{\text{total}}(\text{Int}) = y_0[h\pi^{1/2}/2(\ln 2)^{1/2}] + u^2(2\theta) y_0^2 (2\pi \ln 2)^{1/2}/h. \tag{20}$$

The ratio $\left\{\sum_{i=1}^{n} [y_i' u(2\theta)]^2\right\}^{1/2} \Big/ u_{\text{Poisson}}(\text{Int})$ is calculated as

$$\frac{\left\{\sum_{i=1}^{n} [y_i' u(2\theta)]^2\right\}^{1/2}}{u_{\text{Poisson}}(\text{Int})} = \left[\frac{u^2(2\theta) y_0^2 (2\pi \ln 2)^{1/2}/h}{y_0 h \pi^{1/2}/2(\ln 2)^{1/2}}\right]^{1/2}. \tag{21}$$

Using v defined in (16) for 2θ at steepest slope, we find

$$\frac{\left\{\sum_{i=1}^{n} [y_i' u(2\theta)]^2\right\}^{1/2}}{u_{\text{Poisson}}(\text{Int})} \approx \frac{v}{2^{1/2}} \tag{22}$$

and so the standard uncertainty for the integrated intensity yields

$$u^2_{\text{total}}(\text{Int}) = u^2_{\text{Poisson}}(\text{Int})(1 + v^2/2). \tag{23}$$

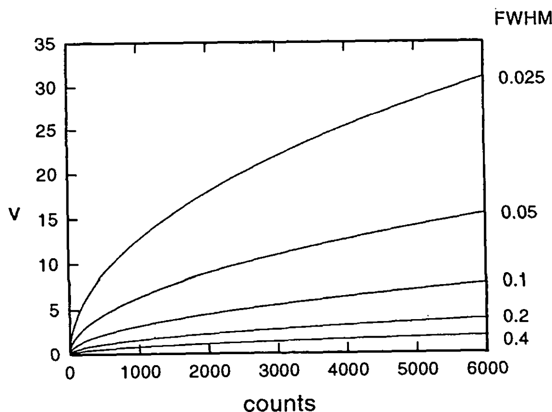

Fig. 5. Ratio v [equation (12)] at the position of steepest slope in a Gaussian profile for $u(2\theta) = 0.005°$. v is the ratio of two contributions to the standard uncertainty in intensity: $y_i'[u(2\theta)]$ depending on the error in angular position divided by u_{Poisson}. The dependence of v on intensity is given for Gaussians with different values of FWHM: 0.025, 0.05, 0.1, 0.2 and 0.4°, respectively.

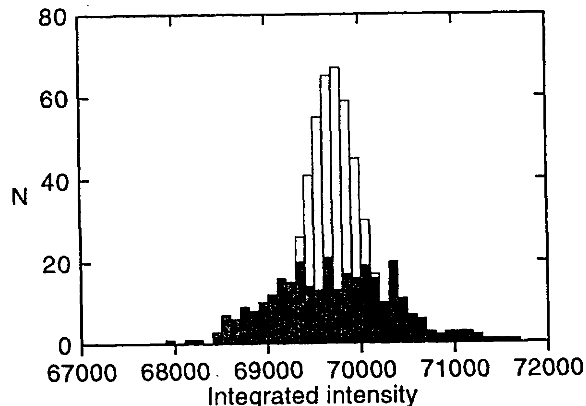

Fig. 6. Histogram of the integrated intensities of 311 Si 220 measurements, $\bar{I} = 69\,714$, $u_{\text{total}}(\text{Int}) = 670$ [see equation (23)] and theoretical purely Poisson distributed intensity with $\bar{I} = 69\,714$, $u_{\text{Poisson}}(\text{Int}) = 264$ (light).

It is evident that the correction for the integrated intensity is of the same order of magnitude as the correction at the angle of steepest slope.

The validity of (23) was checked using the integrated intensities of the 447 Si 220 reflections. These measurements were processed in two groups, comprising, respectively, profiles 1–135 and 136–447 because the set-up was readjusted during the measurements. Fig. 6 shows the histogram of the integrated intensities of 311 Si 220 reflections, each scaled upon the mean monitor count rate, with the standard uncertainty $u_{\rm total}({\rm Int}) = 670$, defined as $u_{\rm total}({\rm Int}) = (1/310)\sum_{\mu=136}^{447}(I_\mu - \bar{I})^2$. Using the standard uncertainty of Poisson statistics $u^{\rm Int}_{\rm Poisson} = 264$, calculated from the mean value of the intensity $\bar{I} = 69\,714$, equations (23) and (18) yield a standard uncertainty in angular position of $u(2\theta) = 0.0011°$. The same evaluation for reflections 1–135 yields $u(2\theta) = 0.0013°$.

5. Conclusions

This analysis of the influence of the weighting system on statistic qualifiers shows that a realistic assumption of the uncertainties during the experiment is the prerequisite to judge the model by statistic tests. Very valuable is the combination of χ^2, given here as N_σ, and the Durbin–Watson test, as they are not correlated. We see also that uncertainties assumed for the data correlate to some extent with the model, if the test relies on N_σ only. This causes the difference between $u(2\theta) = 0.0011°$ found from (23), using the FWHM and the intensity of the Si 220 reflection, and $u(2\theta) = 0.00375°$ found by minimizing N'_σ [equation (11)]. Nevertheless, we conclude that in diffractometry the typical mechanical accuracy of the counter gear of $0.001 < u(2\theta) < 0.004°$ gives a good estimate for $u(2\theta)$. In the case of fixed multicounter arrangements, the standard uncertainty of 2θ results from the deviation of the actual position of each channel from its calculated value. For neutron diffraction with one counter and a FWHM of typically $0.2°2\theta$, only for peak intensities <400 counts is the standard uncertainty in intensity caused by $u(2\theta)$ less than the Poisson statistics (Fig. 5). If the intensities increase, either by addition of several channels or by increasing measuring time, the slope increases because the line width remains constant and $u(2\theta)$ causes the major contribution to the intensity statistics. This explains the well known fact (Hill, 1993) that with increasing measuring time the statistical qualities of the data (*e.g.* GoF) – using Poisson statistics alone – become worse. So, in programs using step-scan data, the standard uncertainty of each intensity value should be given as input data to allow the adaptation of the weighting scheme to the individual experiment (Ritter *et al.*, 1996). However, if a structure refinement program allows a modification of the weighting scheme for the integrated intensity I, comparison with (23) shows that an expression like

$$w = 1/(I + kI^2) \tag{24}$$

with constant k is an approximation allowing for the influence of the standard uncertainty in the angular position.

Financial help by the DFG (project Ih 9/3-3 and Ih 9/3-4) as well as by the BMBF (project 05 647 VTA) is gratefully acknowledged.

References

Bérar, J.-F. & Lelann, P. (1991). *J. Appl. Cryst.* **24**, 1–5.
Durbin, J. & Watson, G. S. (1950). *Biometrika*, **37**, 409–428.
Durbin, J. & Watson, G. S. (1951). *Biometrika*, **38**, 159–178.
Durbin, J. & Watson, G. S. (1971). *Biometrika*, **58**, 1–19.
Flack, H. D. & Vincent, M. G. (1980). *Acta Cryst.* A**36**, 495–496.
Hill, R. J. (1993). *The Rietveld Method*, edited by R. A. Young, ch. 5. Oxford University Press.
Hill, R. J. & Flack, H. D. (1987). *J. Appl. Cryst.* **20**, 356–361.
Hill, R. J. & Madsen, I. C. (1984). *J. Appl. Cryst.* **17**, 297–306.
Hill, R. J. & Madsen, I. C. (1986). *J. Appl. Cryst.* **19**, 10–18.
Ihringer, J. (1995*a*). *Key Engineering Materials*, Vols. 101–102, *Diffusionless Phase Transitions in Oxides*, edited by C. Boulesteix, pp. 3–40. Aedermansdorf, Switzerland: Trans Tech Publications.
Ihringer, J. (1995*b*). *J. Appl. Cryst.* **28**, 618–619.
Ihringer, J. & Appel, W. (1984). *Rev. Sci. Instrum.* **55**, 1978–1979.
Ihringer, J. & Röttger, K. (1993). *J. Phys. D*, **26**, A32–A34.
Ihringer, J. & Röttger, K. (1994). *J. Appl. Cryst.* **27**, 1063–1065.
Ihringer, J. & Röttger, K. (1997). *Institut fuer Kristallographie, Tuebingen*, http://www.uni-tuebingen.de/uni/pki/.
Lehmann, M. S., Christensen, A. N., Fjellväg, H., Feidenhans'l, R. & Nielsen, M. (1987). *J. Appl. Cryst.* **20**, 123–129.
Parrish, W. & Wilson, A. J. C. (1992). *International Tables for Crystallography*, Vol. C, edited by A. J. C. Wilson, p. 428. Dordrecht: Kluwer Academic Publishers.
Prince, E. (1993). *The Rietveld Method*, edited by R. A. Young, ch. 3. Oxford University Press.
Rietveld, H. M. (1967). *Acta Cryst.* **22**, 151–152.
Rietveld, H. M. (1969). *J. Appl. Cryst.* **2**, 65–71.
Ritter, H., Ihringer, J., Maichle, J. K. & Prandl, W. (1996). *SIMREF2.4. Program for the Simultaneous Structure Refinement of Neutron, Synchrotron and X-ray Powder Diffraction Patterns.* University of Tübingen, Germany. http://www.uni-tuebingen.de/uni/pki/simref/simref.html.
Sakata, M. & Cooper, M. J. (1979). *J. Appl. Cryst.* **12**, 554–563.
Schwarzenbach, D., Abrahams, S. C., Flack, H. D., Gonschorek, W., Hahn, Th., Huml, K., Marsh, R. E., Prince, E., Robertson, B. E., Rollet, J. S. & Wilson, A. J. C. (1989). *Acta Cryst.* A**45**, 63–75.
Willis, B. T. M. & Albinati, A. (1992). *International Tables for Crystallography*, Vol. C, edited by A. J. C. Wilson, pp. 625–626. Dordrecht: Kluwer Academic Publishers.
Young, R. A. (1993). *The Rietveld Method*, edited by R. A. Young, pp. 9–10. Oxford University Press.